Widespread spatial integration in primary somatosensory cortex

Jamie L. Reed*, Pierre Pouget†, Hui-Xin Qi†, Zhiyi Zhou‡, Melanie R. Bernard‡, Mark J. Burish*§, John Haitas†, A. B. Bonds¶‖, and Jon H. Kaas†‖**

*Neuroscience Graduate Program, Vanderbilt Brain Institute, U1205 Medical Center North, Vanderbilt University, Nashville, TN 37235-2050; Departments of ‡Biomedical Engineering and ¶Electrical Engineering and Computer Science, Vanderbilt University, Nashville, TN 37235; †Department of Psychology and ‖Center for Integrative and Cognitive Neuroscience and Vanderbilt Vision Research Center, Vanderbilt University, Nashville, TN 37203; and §Medical Scientist Training Program, Vanderbilt University School of Medicine, Nashville, TN 37232

Contributed by Jon H. Kaas, April 21, 2008 (sent for review February 19, 2008)

Tactile discrimination depends on integration of information from the discrete receptive fields (RFs) of peripheral sensory afferents. Because this information is processed over a hierarchy of subcortical nuclei and cortical areas, the integration likely occurs at multiple levels. The current study presents results indicating that neurons across most of the extent of the hand representation in monkey primary somatosensory cortex (area 3b) interact, even when these neurons have separate RFs. We obtained simultaneous recordings by using a 100-electrode array implanted in the hand representation of primary somatosensory cortex of two anesthetized owl monkeys. During a series of 0.5-s skin indentations with single or dual probes, the distance between electrodes from which neurons with synchronized spike times were recorded exceeded 2 mm. The results provide evidence that stimuli on different parts of the hand influence the degree of synchronous firing among a large population of neurons. Because spike synchrony potentiates the activation of commonly targeted neurons, synchronous neural activity in primary somatosensory cortex can contribute to discrimination of complex tactile stimuli.

classical receptive field | neuronal synchrony | primate | two-point stimulation | Utah array

Humans and other primates use their hands to make tactile discriminations that guide choices and actions. The vast majority of these choices are based on stimuli that are presented to sites across the hand or hands. Transformation of these scattered information sources from receptors in distinct patches of skin into one percept presumes integration within the central nervous system. This integration could occur at several levels, but here we consider the primary somatosensory cortex (S1 or area 3b). Though area 3b contains a detailed somatotopic representation of the hand and neurons with small receptive fields (RFs), considerable integration across hand locations may occur at this level via horizontal connections within area 3b.

One way of examining neuronal interactions is through spike timing synchrony. When the spikes of two neurons occur together more often than expected by chance, we can infer that those neurons are part of the same local network. The two neurons may receive a common input that drives the synchronous firing, or the neurons may be synaptically connected. Our focus was on quantifying integration in anesthetized owl monkeys (*Aotus trivirgatus*) in the form of spike synchrony of neuronal activity in layers 2/3 of S1. Analysis of firing rate will be presented elsewhere.

Using a 100-electrode array (Cyberkinetics) covering 4 mm × 4 mm of cortical area (Fig. 1 *A* and *B*), we examined sensory input integration in the area 3b hand representation by focusing on correlations in spike timing in pairs of neurons responding to the same or different stimulus probes (1-mm-diameter contact surface). We examined interactions across, rather than within, digit and palm pads to determine the extent of spatial integration in the area 3b hand representation.

Correlations between neurons have been proposed as a biophysical mechanism by which neurons at lower levels in processing hierarchies more effectively increase the responsiveness of neurons at higher levels (e.g., refs. 1 and 2). In the primate somatosensory system, spike timing correlations have been studied primarily in secondary somatosensory cortex (S2) in awake macaque monkeys performing attention tasks (e.g., refs. 3 and 4) because firing rate changes without spike synchrony changes have been associated with attention in S1 (5). Here, we examined spike synchrony in S1 of anesthetized owl monkeys. Rather than studying synchrony as a neural correlate of attention, we studied the role of spike synchrony as a low-level correlate of stimulus processing and integration. We examined spike timing synchrony by using joint peristimulus time histogram analysis (JPSTH) based on methods from Aertsen and colleagues (6). The analysis focuses on the subset of spike timing correlations that likely arise from functional connections, rather than correlations due to stimulus-related changes in firing rate. In particular, our purpose is to infer the influence of common input and lateral connections in area 3b. The data presented include dual-site stimulation on nonadjacent hand locations, as stimulus interactions between nonadjacent digits would be strict indicators of effects from "beyond the classical receptive field" (7).

Neurons with overlapping RFs might be expected to show spike timing correlations based on common input and/or synaptic connections. Neurons with nonoverlapping RFs might be less likely to share information and fire synchronous spikes. Simultaneous recordings in S1 and S2 in cats revealed that neurons with synchronized spike times tended to have overlapping RFs, whereas the pairs that did not show synchrony tended to have nonoverlapping RFs (8). However, recent studies in visual cortex have led to the proposal that synchrony is related to stimulus properties (e.g., refs. 9 and 10). Therefore, we tested whether we could drive synchronous firing between neurons with nonoverlapping RFs responding to stimulation on nonadjacent locations, as a signal of information integration beyond the classical RF.

Results

Recordings were obtained by using a 100-electrode array implanted in layers 2/3 of S1 of two anesthetized owl monkeys; one or two sites on the hand were stimulated. We selected 182 units from the two monkeys based on response criteria to the stimulation conditions (see *Materials and Methods*). From monkey 1,

Author contributions: J.L.R., H.-X.Q., and J.H.K. designed research; J.L.R., H.-X.Q., Z.Z., M.R.B., and M.J.B. performed research; P.P., J.H., and A.B.B. contributed new reagents/analytic tools; J.L.R., P.P., and J.H. analyzed data; and J.L.R., P.P., and J.H.K. wrote the paper.

The authors declare no conflict of interest.

**To whom correspondence should be addressed at: Department of Psychology, Vanderbilt University, 301 Wilson Hall, 111 21st Avenue South, Nashville, TN 37203. E-mail: jon.h.kaas@vanderbilt.edu.

This article contains supporting information online at www.pnas.org/cgi/content/full/0803800105/DCSupplemental.

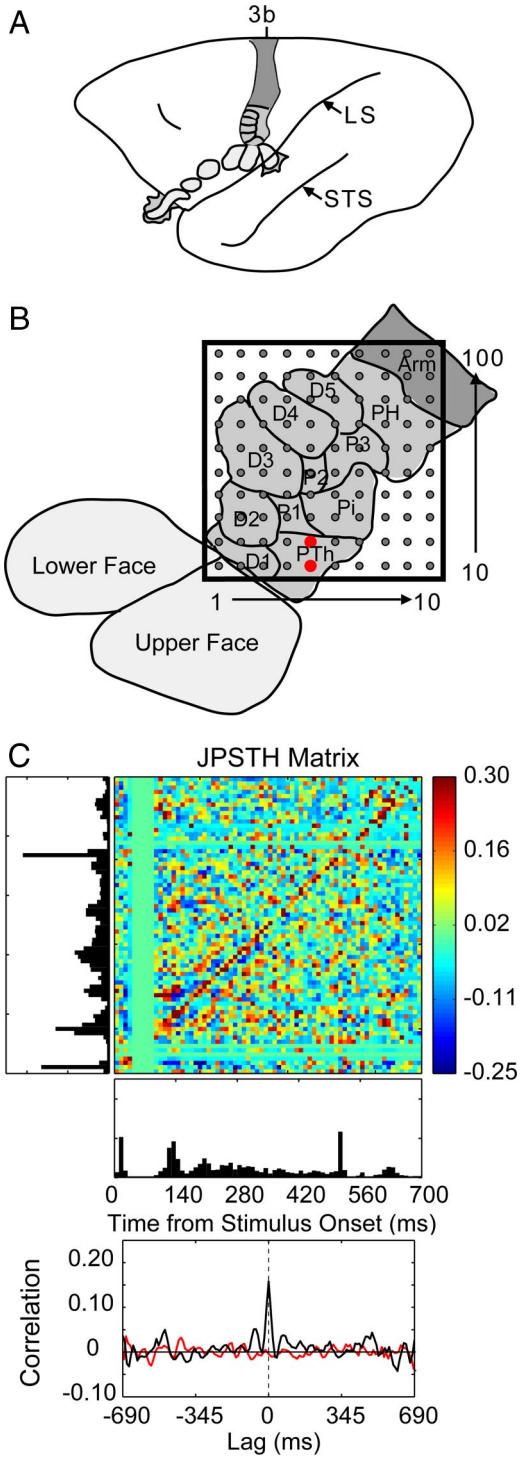

Fig. 1. An example of correlated spike activity recorded from two adjacent electrodes in monkey 1. (*A*) A lateral schematic view of an owl monkey brain with area 3b shaded. Subdivisions representing the face and hand are outlined, including those that cannot be seen from a surface view. LS, lateral sulcus; STS, superior temporal sulcus. (*B*) The location of the array within the area 3b hand representation. The approximate representations of the digits (D1–5) and the digital (P1–3), thenar (PTh), hypothenar (PH) and insular (Pi) pads of the hand are identified and outlined. The red dots mark the electrodes where the two neurons were recorded for the analysis shown in *C*. Both neurons had RFs on the PTh pad. (*C*) An example of the spike timing synchrony of units recorded from adjacent electrodes. Two probes simultaneously indented the skin on the PTh and P1 pads. Spike synchrony between the two neurons is shown in the normalized joint peristimulus time histogram, the JPSTH matrix. The two PSTHs of the responses to 100 repetitions of 0.5-s skin indentations are shown to the left and below the matrix, with the cross-correlation histogram derived from the JPSTH analysis directly below. The colored pixels in the JPSTH matrix represent the magnitude of the normalized correlation at different lag times over a poststimulus time of 700 ms. Strong spike synchrony occurred around a 0-ms lag time throughout the period. The cross-correlation histogram (black) revealed a peak correlation of 0.16 that exceeded the mean correlation from the shuffled trials (red).

28 units were classified as single units and 66 were multiunits. From monkey 2, 42 units were single units and 46 were multiunits. Across all stimulation conditions, this resulted in 1,244 single unit pairs and 2,476 multiunit pairs for spike timing analysis. Paired nonadjacent locations selected for stimulation included digit 1 (D1) with digit 3 (D3), digit 2 (D2) with digit 4 (D4), and the thenar palm pad (PTh) with palm pad 2 (P2). We obtained responses from 50 single units and 63 multiunits while analyzing 316 single unit pairs and 473 multiunit pairs for synchrony. Only one unit was selected per electrode for analysis so that no spike timing correlations were performed between units from the same electrode. Thus, it is unlikely that spike correlations were calculated between contaminated spikes (11). Our measure of synchrony was the peak magnitude of correlation between pairs of neurons based on JPSTH analysis with spike trains aligned at the start of a 0.5-s skin indentation. Pairs with significant correlations showed synchronous spiking during the sustained skin indentation, not only at stimulus onset and removal (Fig. 1*C*).

Multielectrode Recordings Indicate Widespread Stimulus Effects. Responses of area 3b neurons to 0.5-s skin indentations within the minimal RF (based on traditional mapping techniques) included a sharp onset response followed by some response depression, a variable level of maintained activity, and often an off response, depression, and a return to prestimulus levels of spontaneous activity. Neurons included in the analysis showed sustained activity in response to the 0.5-s stimulation on at least one of the hand locations in the recording conditions (see *Materials and Methods*). Although rapidly adapting neuron types with low levels of spontaneous activity and transient responses to stimulation were recorded, these were not included in the analysis because the JPSTH calculation requires many spikes to obtain an estimate of spike timing synchrony (6, 11, 12). The recorded responses were similar to those reported previously from area 3b neurons in monkeys (e.g., refs. 13 and 14).

We found correlated spike times between pairs of neuron units recorded from adjacent electrodes (0.4 mm center-to-center distance), as well as from distant electrodes (>2 mm apart). An example of the extent of correlations when a single site on the PTh was stimulated repeatedly is shown in Fig. 2. A representation of the peak firing rate for the subset of units analyzed for synchrony is shown in conjunction with the peak correlations between unit pairs.

Quantification of Spatial Integration Across Area 3b Indicates Extensive Interactions. The proportion of unit pairs with synchronous spike timing decreased when two sites were stimulated compared to single-site stimulation. During single-site stimulation, 49.6% of the pairs recorded showed synchrony in their spike timing. During dual-site stimulation, 28.2% of the pairs were synchronized. For both single- and dual-site stimulation conditions, the proportion of correlated pairs decreased as the cortical distance separating the two units increased (Table 1). When one site was stimulated, 58.7% of the neuron pairs recorded <1.0 mm apart had significant spike timing correlations. This proportion dropped to 16.7% for pairs that were separated by 4.0–5.0 mm. When two nonadjacent sites were stimulated, 35.6% of the neuron pairs recorded <1.0 mm apart were synchronized. This

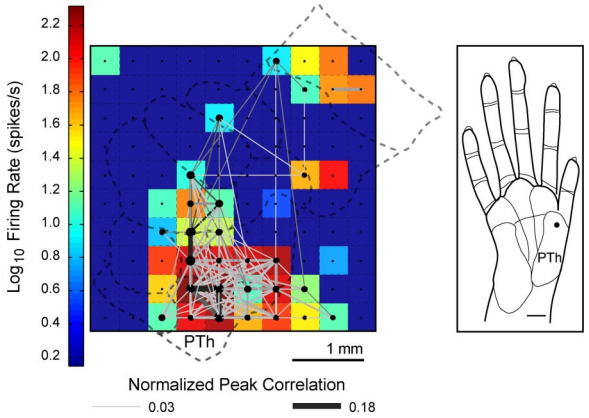

Fig. 2. An example of widespread spike timing correlations and firing activity. Significant peak correlations across the sampled neuron-units in the 100-electrode array are displayed in a grid. A color map representing the peak firing rates of the units is overlaid on a schematic of the area 3b hand representation to indicate the approximate spatial locations of the electrodes. Shown is one example from monkey 1 when a single site on the thenar (PTh) palm was stimulated repeatedly (100 trials). Dots indicate electrode sites and significant correlations between units are represented by the lines connecting the dots. The size of the dots and the thickness of the connecting lines are visual representations of the peak magnitude of the correlation. Each colored box represents the peak firing rate of a unit at one electrode site. Peak firing rates are shown for those units included in the synchrony analysis. Dark blue squares indicate electrodes not analyzed for spike synchrony because units did not show sustained responses to stimulation.

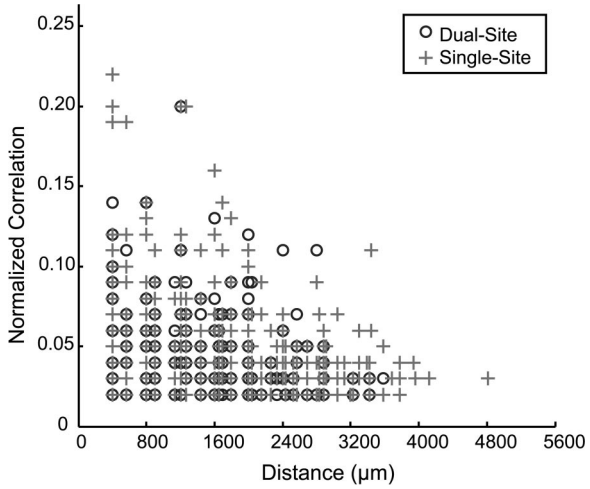

Fig. 3. Relationship of spike timing peak correlation magnitude to the distance between electrodes. The normalized, significant peak correlation magnitudes are plotted as a function of distance between the correlated unit pairs for monkeys 1 and 2 when nonadjacent sites were simultaneously stimulated (Dual-Site) or when single sites were stimulated as controls (Single-Site).

proportion dropped to 7.5% for pairs separated by 3.0–4.0 mm. We speculate that information provided by synchronous activity became more specific when two sites were stimulated.

As a next step, we examined the relationship of the distance between correlated pairs and the magnitude of the peak correlation. The data were summarized for both monkeys in a scatter plot (Fig. 3) to determine whether strong correlations tended to occur between neurons on adjacent electrodes. We found a weak, but significant trend for stronger correlations occurring between neurons recorded from nearby electrodes when a single site was stimulated ($r = -0.2247$, $P < 0.0001$, $n = 533$), as well as when two nonadjacent sites were simultaneously stimulated ($r = -0.2048$, $P = 0.006$, $n = 179$). We found that significant correlations occurred between neurons recorded from distant electrodes (>2 mm apart).

Discussion

One might expect that spatial integration by area 3b neurons is very limited, because RFs have been consistently described as restricted in size, usually confined to part of a phalanx of a single digit or palm pad (15–17), and appear uniformly excited when probed with punctate stimuli (18–20). Studies indicate that inhibitory surrounds of area 3b neurons in hand cortex do not substantially enlarge the RF area (15, 19, 20). Here, we show that traditional depictions of RFs do not reflect the extent of integration that occurs in area 3b.

The ability to record from 100 electrodes simultaneously allows us to examine responses and spike synchrony across a large extent within a single cortical area or between areas. Our experiment, using tactile stimulation of nonadjacent hand sites of anesthetized owl monkeys, demonstrates the widespread spatial integration of sensory inputs present in the area 3b hand representation. When even a single site was stimulated with repeated skin indentations, neurons on numerous electrodes responded to the 1 mm diameter stimulus. These results are in agreement with findings in which chronic multisite recordings in owl monkey somatosensory cortex areas 3b, 2, and S2 showed widespread activity in response to single-site tactile stimulation and evidence for ensemble coding of stimulus location using firing rates (21). Spike timing correlations occurred between neurons separated by millimeters of cortex, beyond the predicted extent of the representation of the palm pad location at that site (Fig. 2), suggesting a functional connectivity that has been largely overlooked.

Correlated firing among neurons can occur through four basic mechanisms: (*i*) a common input arriving nearly simultaneously to the neurons; (*ii*) lateral connections within cortex; (*iii*)

Table 1. Proportions of correlated pairs across cortical distance in S1

	Cortical distance, mm						
Site stimulation	0–1.0	1.0–2.0	2.0–3.0	3.0–4.0	4.0–5.0	5.0–6.0	Total
Single							
Recorded pairs, *n*	264	378	321	100	12	0	1,075
Synchronized pairs, *n*	155	205	134	37	2	0	533
Proportion, %	58.7	54.2	41.7	37.0	16.7	—	49.6
Dual							
Recorded pairs, *n*	146	223	192	67	6	0	634
Synchronized pairs, *n*	52	75	47	5	0	0	179
Proportion, %	35.6	33.6	24.5	7.5	0	—	28.2

—, not applicable.

responses in unconnected neurons to a common stimulus; and (*iv*) statistical coincidence due to firing rate. Our corrections in the correlation calculations remove or reduce the impact of *iii* and *iv*, although "uncorrected correlations" likely have roles in stimulus processing (12). Thus, we are left to determine whether the correlations we find are due to a common input or lateral connections. We recorded from neuron pairs with the same or overlapping RFs, which are likely to receive a common activating input, as well as have strong lateral connections (e.g., refs. 22 and 23). These neurons were in close proximity (adjacent electrodes, 0.4 mm apart). Significant spike correlations also occurred for neurons with nonoverlapping RFs across larger regions of cortex (>2 mm apart). It is unlikely that synchronies between neuron pairs with dissimilar RFs induced by stimulating two nonadjacent digits simultaneously are due to a common thalamocortical input, because the densest thalamocortical projections are topographically matched, although a few projections spread across distinct representations in area 3b of owl monkeys (24, 25). Lateral projections extend across segregated digit representations in monkey area 3b (e.g., refs. 26–28). Thus, we propose that common thalamic inputs, together with dense lateral connections, result in strong correlations between neurons across a localized area of cortex in which neurons have overlapping RFs, whereas longer and less dense intrinsic lateral connections (24–28) contribute to weaker correlations that spread across a larger area. An additional source of correlated activity between distant neurons could be common feedback connections from higher-order somatosensory areas with large RFs.

Evidence for Widespread Correlated Neural Assemblies in Area 3b. Recent studies have shown attention-induced changes in spike time synchrony between pairs of neurons in primate somatosensory cortex (e.g., refs. 3–5 and 29). To a large extent, such synchronies have been interpreted as a high-level integration process based on feedback connections from higher levels, despite evidence for robust synchrony in anesthetized preparations (9, 10, 30–34). Synchrony in unconscious animals implies specific anatomical connectivity between neurons, and populations of neurons, and emphasizes that higher levels of integration must consider low-level integration.

Our results, using paired stimuli on multiple locations across the hand, expand previous correlation studies in somatosensory cortex that found that neurons with overlapping RFs have strong correlations when probed with single stimuli inside the RF and moving stimulation (e.g., 32–34). Similar to findings in cat S2 (32), we found that the magnitude of correlated activity decreased with increased electrode distance (Fig. 3). However, the spatial distance between correlated neurons was surprising, as significant correlations occurred between neurons separated by over 2 mm (Table 1 and Fig. 3). As suggested by Alloway and colleagues (33), we found that spike timing synchrony in S1 may be related to stimulus properties in anesthetized animals, indicating that low-level integration processes play an important role in neural coding, in addition to the role played in higher-level processes (such as attention).

In conclusion, we have shown evidence for extensive sensory input integration in S1 cortex of anesthetized owl monkeys. Traditional minimal RF (mRF) mapping is only the "tip of the iceberg" in terms of reflecting the actual stimulus interactions that take place in the area 3b hand representation. Interactions extend across nonadjacent digit sites, despite the lack of RF mapping studies in primates showing such large fields in area 3b. The differences in our findings compared with traditional RF mapping can be explained in part by our stimulus. We use a suprathreshold stimulus to drive responses, whereas RF mapping is typically done with near-threshold stimulation. Our suprathreshold stimulus may activate a larger pool of inputs, allowing us to measure interactions that are likely to occur during natural tactile stimulation. Using our method, we found sensory input integration across regions much larger than the small RFs and discrete digit representations predict. We propose that neurons, even at the first level of somatosensory cortex, participate in global aspects of stimulus processing, on which higher-level processing is based.

Materials and Methods

Preparation. Two adult owl monkeys (1 kg) were prepared for electrophysiological recording from primary somatosensory cortex under the guidelines established by the National Institutes of Health and the Animal Care and Use Committee at Vanderbilt University. Animals were anesthetized with propofol and N_2O and paralyzed with vecuronium bromide. See supporting information (SI) for detailed methods. A small craniotomy was made over the primary somatosensory cortex, and the dura was removed. The electrode array was inserted into the cortex pneumatically to a depth of 600 μm, such that electrode tips are expected to be within layers 2/3. The opening was covered with agar mixed with Ringer's solution to provide stability. Similar methods have been described elsewhere (10, 35).

Stimulation Procedures. Computer-controlled stimuli were generated in a custom-designed Visual Basic program and executed with two independent force- and position-feedback controlled motor systems (300B; Aurora Scientific). Round Teflon probes 1 mm in diameter delivered tactile stimuli to the glaborous hand. Stimuli consisted of pulses that indented the skin 0.5 mm for 0.5 s, followed by a 2.0-s period off the skin, repeated for 255–300 s. These parameters allowed us to detect responses to stimulus on and off times and classify phasic or sustained responses (14). Paired sites were selected for stimulation and the pulses were delivered simultaneously. Single-site control stimuli were delivered to each of the sites in the pair before simultaneous stimulation. For practical purposes, reference units were identified and probes were positioned so that one probe was inside and one probe was outside the mRF of the reference neuron. Procedures for mRF mapping have been published elsewhere (36–38). See *SI Text* for details regarding mRF mapping and stimulation procedures.

Data Acquisition. Recordings were made by using the 10 × 10 Utah array and the Bionics Data Acquisition System (Cyberkinetics Neurotechnology Systems). The signals on each channel were amplified 5,000 times and band-pass filtered between 250 Hz and 7.5 kHz. The threshold for each electrode was automatically set for 3.25-times the mean activity and the waveforms were sampled at 30 kHz for 1.5-ms windows (10).

Histology. After data collection, animals were perfused and the brains were prepared for histological analysis as described previously (36). The cortex was flattened and cut frozen at 40 μm. Sections were processed for myelin to aid in determining the electrode sites relative to the area 3b hand representation. Fig. S1 shows the tissue quality that may be obtained by using the 100-electrode array.

Data Analysis. ***Spike sorting and data selection.*** Spike signals were sorted offline with an automatic spike classification program for Matlab (Mathworks) based on the t-distribution expectation maximization algorithm (39). All recordings for a given stimulation series were sorted together to standardize sorting across recordings. We reviewed each recording with a second spike sorter program, Plexon Offline Sorter (Plexon). See *SI Text* and Fig. S2 for sorting details. We used the Plexon software to verify the quality of unit isolation such that single units had refractory periods of $\geq$1.2 ms, P values of $\leq$0.05 for multivariate ANOVA related to cluster separation, and distinct waveform amplitudes and shapes when compared with other activity on the same electrode (40). Single units and multiunits were grouped separately. In each monkey, several of the electrodes recorded single unit activity (45 electrodes and 65 electrodes for monkeys 1 and 2, respectively); however, not all single units responded significantly under each stimulus condition. Only units that responded to a given stimulus condition with peak firing rates above the upper 99% confidence limit of the expected mean firing rate were included in the analyses for that condition. Confidence limits were calculated with NeuroExplorer software (Nex Technologies) based on the assumption that the spike counts have a Poisson distribution.

Additionally, neurons included in the analysis showed sustained activity in at least one of the stimulus conditions such that spiking activity was maintained during the 0.5-s skin indentation. In practice, both of the following criteria had to be reached for a unit to be included in the correlation analysis. The activity between 100 and 500 ms after stimulus onset must have reached

the upper 95% confidence limit of the mean firing rate for three or more consecutive 1-ms bins, and the activity within this 400-ms period must have exceeded the expected mean firing rate for at least fifty 1-ms bins. Units showing only rapidly adapting response properties typically had relatively low spike counts, which makes the interpretation of JPSTH analysis difficult or even biased, so these units were excluded from analysis. Finally, we selected one unit per electrode for JPSTH analysis, choosing single units over multiunits when possible.

Spike time synchrony. Spike synchrony between pairs of neurons was measured from the cross-correlation histogram derived from the JPSTH analysis with all spike trains aligned on the onset of skin indentation following previous conventions (6, 11, 41). See *SI Text* for detailed methods. We compared the peak correlation value from the cross-correlation histogram derived from the normalized JPSTH of neurons across stimulus conditions. Fig. S3 shows examples of JPSTHs during stimulation and no stimulation; however, the very low spike counts in anesthetized animals in absence of tactile stimulation typically did not reach an appropriate number of spikes for use of the JPSTH calculation (6, 11, 12) and were not analyzed.

We tallied the proportion of synchronized neuron pairs to the total recorded pairs for groups of cortical distances separating the neurons in the pair. To represent the relationship of the electrode distance between the correlated neurons with the magnitude of the spike timing correlations, we measured the distance between electrodes and the correlation strength for a given stimulus condition. We examined these paired values of distance and spike timing correlation magnitude in a scatter plot and performed linear regression on the population summary to obtain the correlation coefficient using Matlab.

ACKNOWLEDGMENTS. We thank Dr. Jeff Schall for comments and insight regarding development of analysis methods and Dr. O. Gharbawie and C. Camalier for help collecting data from case 2. This work was supported by the James S. McDonnell Foundation (J.H.K.) and National Institutes of Health Grants NS16446 (to J.H.K.), F31-NS053231 (to J.L.R.), EY014680–03 (to A.B.B.), T32-GM07347 (to M.J.B.), P30-EY08126, and P30-HD015052.

1. Azouz R, Gray CM (2000) Dynamic spike threshold reveals a mechanism for synaptic coincidence detection in cortical neurons *in vivo*. *Proc Natl Acad Sci USA* 97:8110–8115.
2. Salinas E, Sejnowski TJ (2001) Correlated neuronal activity and the flow of neural information. *Nat Rev Neurosci* 2:539–550.
3. Niebur E, Hsiao SS, Johnson KO (2002) Synchrony: A neuronal mechanism for attentional selection? *Curr Opin Neurobiol* 12:190–194.
4. Roy A, Steinmetz PN, Hsiao SS, Johnson KO, Niebur E (2007) Synchrony: A neural correlate of somatosensory attention. *J Neurophysiol* 98:1645–1661.
5. Hsiao SS, O'Shaughnessy DM, Johnson KO (1993) Effects of selective attention on spatial form processing in monkey primary and secondary somatosensory cortex. *J Neurophysiol* 70:444–447.
6. Aertsen AMHJ, Gerstein GL, Habib M, Palm G (1989) Dynamics of neuronal firing correlation: Modulation of ''effective connectivity''. *J Neurophysiol* 61:900–917.
7. Allman J, Miezin F, McGuinness E (1985) Stimulus specific responses from beyond the classical receptive field: Neurophysiological mechanisms for local-global comparisons in visual neurons. *Annu Rev Neurosci* 8:407–430.
8. Roy SA, Dear SP, Alloway KD (2001) Long-range cortical synchronization without concomitant oscillation is in the somatosensory system of anesthetized cats. *J Neurosci* 21:1795–1808.
9. Samonds JM, Zhou Z, Bernard MR, Bonds AB (2006) Synchronous activity in cat visual cortex encodes collinear and cocircular contours. *J Neurophysiol* 95:2602–2616.
10. Samonds JM, Allison JD, Brown HA, Bonds AB (2003) Cooperation between Area 17 neuron pairs enhances fine discrimination of orientation. *J Neurosci* 23:2416–2425.
11. Gerstein GL (2000) Cross-correlation measures of unresolved multi-neuron recordings. *J Neurosci Methods* 100:41–51.
12. Gerstein GL, Bedenbaugh P, Aertsen AMHJ (1989) Neuronal assemblies. *IEEE Trans Biomed Eng* 36:4–14.
13. Mountcastle VB, Talbot WH, Sakata H, Hyvarinen J (1969) Cortical neuronal mechanisms in flutter-vibration studied in unanesthetized monkeys. Neuronal periodicity and frequency discrimination. *J Neurophysiol* 32:452–484.
14. Sur M, Wall JT, Kaas JH (1984) Modular distribution of neurons with slowly adapting and rapidly adapting responses in area 3b of somatosensory cortex in monkeys. *J Neurophysiol* 51:724–744.
15. DiCarlo JJ, Johnson KO, Hsiao SS (1998) Structure of receptive fields in area 3b of primary somatosensory cortex in the alert monkey. *J Neurosci* 18:2626–2645.
16. Iwamura Y, Tanaka M, Sakamoto M, Hikosaka O (1983) Functional subdivisions representing different finger regions in area 3b or the first somatosensory cortex of the conscious monkey. *Exp Brain Res* 51:315–326.
17. Pons TP, Wall JT, Garraghty PE, Cusick CG, Kaas JH (1987) Consistent features of the representation of the hand in area 3b of macaque monkeys. *Somatosens Res* 4:309–331.
18. Mountcastle VB, Powell TPS (1959) Neural mechanisms subserving cutaneous sensibility, with special reference to the role of afferent inhibition in sensory perception and discrimination. *Bull Johns Hopkins Hosp* 105:201–232.
19. Sripati AP, Yoshioka T, Denchev P, Hsiao SS, Johnson KO (2006) Spatiotemporal receptive fields of peripheral afferents and cortical area 3b and 1 neurons in the primate somatosensory system. *J Neurosci* 26:2101–2114.
20. Sur M (1980) Receptive fields of neurons in areas 3b and 1 of somatosensory cortex in monkeys. *Brain Res* 198:465–471.
21. Nicolelis MAL, *et al*. (1998) Simultaneous encoding of tactile information by three primate cortical areas. *Nat Neurosci* 1:621–630.
22. Burton H, Fabri M (1995) Ipsilateral intracortical connections of physiologically defined cutaneous representations in area 3b and 1 of macaque monkeys: Projections in the vicinity of the central sulcus. *J Comp Neurol* 355:508–538.
23. Gilbert CD (1993) Circuitry, architecture, and functional dynamics of visual cortex. *Cereb Cortex* 3:373–386.
24. Garraghty PE, Pons TP, Sur M, Kaas JH (1989) The arbors of axons terminating in middle cortical layers of somatosensory area 3b in owl monkeys. *Somatosens Mot Res* 6:401–411.
25. Garraghty PE, Sur M (1990) Morphology of single intracellularly stained axons terminating in area 3b of macaque monkeys. *J Comp Neurol* 294:583–593.
26. De Felipe J, Conley M, Jones EG (1986) Long-range focal collateralization of axons arising from corticocortical cells in monkey sensory-motor cortex. *J Neurosci* 6:3749–3766.
27. Manger PR, Woods TM, Muñoz A, Jones EG (1997) Hand/face border as a limiting boundary in the body representation in monkey somatosensory cortex. *J Neurosci* 17:6338–6351.
28. Fang PC, Jain N, Kaas JH (2002) Few intrinsic connections cross the hand-face border of area 3b of new world monkeys. *J Comp Neurol* 454:310–319.
29. Steinmetz PN *et al*. (2000) Attention modulates synchronized neuronal firing in primate somatosensory cortex. *Nature* 404:187–190.
30. Bruno RM, Sakmann B (2006) Cortex is driven by weak but synchronously active thalamocortical synapses. *Science* 312:1622–1627.
31. Eggermont JJ (2006) Properties of correlated neural activity clusters in cat auditory cortex resemble those of neural assemblies. *J Neurophysiol* 96:746–764.
32. Alloway KD, Zhang M, Dick SH, Roy SA (2002) Pervasive synchronization of local neural networks in the secondary somatosensory cortex of cats during focal cutaneous stimulation. *Exp Brain Res* 147:227–242.
33. Roy SA, Alloway KD (1999) Synchronization of local neural networks in the somatosensory cortex: A comparison of stationary and moving stimuli. *J Neurophysiol* 81:999–1013.
34. Alloway KD, Johnson MJ, Wallace MB (1993) Thalamocortical interactions in the somatosensory system: Interpretations of latency and cross-correlation analyses. *J Neurophysiol* 70:892–908.
35. Xu X, *et al*. (2003) Optical imaging of visually evoked responses in prosimian primates reveals conserved features of the middle temporal visual area. *Proc Natl Acad Sci USA* 101:2566–2571.
36. Jain N, Qi HX, Kaas JH (2001) in Progress in Brain Res, ed Nicolelis MAL, (Elsevier Science, Amsterdam) Vol 130, pp 1–10.
37. Merzenich MM, Kaas JH, Sur M, Lin CS (1978) Double representations of the body surface within cytoarchitectonic areas 3b and 1 in ''SI'' in the owl monkey (*Aotus trivirgatus*). *J Comp Neurol* 181:41–74.
38. Nelson RJ, Sur M, Felleman DJ, Kaas JH (1980) Representations of the body surface in postcentral parietal cortex of Macaca fascicularis. *J Comp Neurol* 192:611–643.
39. Shoham S, Fellows MR, Normann RA (2003) Robust, automatic spike sorting using mixtures of multivariate t-distributions. *J Neurosci Methods* 127:111–122.
40. Nicolelis MAL et al. (2003) Chronic, multisite, multielectrode recordings in macaque monkeys. *Proc Natl Acad Sci USA* 100:11041–11046.
41. Ventura V, Cai C, Kass RE (2005) Statistical assessment of time-varying dependency between two neurons. *J Neurophysiol* 94:2940–2947.